Available online at www.sciencedirect.com
SCIENCE DIRECT®
Journal of Power Sources 126 (2004) 104–111
JOURNAL OF POWER SOURCES
www.elsevier.com/locate/jpowsour

Numerical optimization study of the catalyst layer of PEM fuel cell cathode

Datong Song [a], Qianpu Wang [a], Zhongsheng Liu [a,*], Titichai Navessin [a,b], Michael Eikerling [a,b], Steven Holdcroft [a,b]

[a] *Institute for Fuel Cell Innovation, National Research Council, 3250 East Mall, Vancouver, BC, Canada V6T 1W5*
[b] *Department of Chemistry, Simon Fraser University, Burnaby, BC, Canada V5A 1S6*

Received 11 August 2003; accepted 31 August 2003

Abstract

One- and two-parameter numerical optimization analyses of the cathode catalyst layer of the PEM fuel cell were investigated with the objective of optimizing the current density of the catalyst layer at a given electrode potential. Catalyst design parameters, such as Nafion content, platinum loading, catalyst layer thickness and porosity, were considered. Numerical analysis shows that there is a global, optimal solution for each one-parameter optimization. A global, optimal solution also exists for two-parameter optimizations. The optimal solution and the surface of the local current density as a function of two design parameters are given for each two-parameter optimization. The numerical analyses provided here are useful in the design of cathode catalyst layers.

Keywords: PEM fuel cell; Catalyst layer; Optimization

1. Introduction

Proton exchange membrane (PEM) fuel cells are promising candidates for next generation power sources. They have received much attention in recent years due to their "zero-emission" quality and relative high power density. A PEM fuel cell generally consists of a membrane electrode assembly (MEA), sandwiched between two bipolar plates that allow the introduction of separate reactant gases. The MEA consists of a proton conducting electrolyte membrane sandwiched between two porous gas diffusion layers (GDLs) which have been coated on one side with a thin catalyst layer: it is often prepared from a mixture of catalyst dispersed on carbon black, polyelectrolyte, and a hydrophobic agent. Hydrogen gas diffuses through the anode GDL to the anode catalyst layer and is oxidized to protons. Concurrently, the electrons travel through the electrical circuit to the cathode where, in the presence of protons that have diffused through the membrane, they reduce oxygen that has diffused through the cathode GDL to the cathode catalyst layer.

Many different transport processes occur in different regions of the PEM fuel cell. These include mass transfer of the chemical species (typically hydrogen and oxygen) in the gas channels and porous GDLs, proton and electron transport through the catalyst electrodes and membrane, water transport in different phases through catalyst layers, GDLs and the membrane, and heat transfer. Among these different components and different transport processes, the transport processes in the cathode catalyst layer play a significant role in the performance of the PEM fuel cell because this is the region where the rate limiting chemical reaction takes place and potential power is wasted. Therefore, research on cathode performance has been very active, and many models have been proposed [1–5].

Commercialization requires that the fuel cell achieves its best performance at the lowest cost. Optimal PEM fuel cell performance should be: the highest power output, highest fuel efficiency, while maintaining reliability and durability, and at the lowest cost. Assuming that adequate water and heat management can be achieved, optimal performance will strongly correlate with an optimized cathode catalyst layer.

Optimization by experiment [6–8] is time consuming and costly compared to numerical optimization [9,10], in particular, when more than one variable is involved. On the other hand, the numerical optimization method is inexpensive and can yield global optimization because many parameters can be systematically varied. Qi and Kaufman [8] investigated experimentally the effects of Nafion content and platinum

* Corresponding author. Tel.: +1-604-221-3068.
E-mail address: simon.liu@nrc.gc.ca (Z. Liu).

0378-7753/$ – see front matter.
doi:10.1016/j.jpowsour.2003.08.043

Nomenclature

A	specific reaction surface area per volume of the catalyst layer (cm^{-1})
A_0	catalyst surface area per unit mass of the catalyst ($cm\,g^{-1}$)
c_{O_2}	oxygen concentration in the catalyst layer ($mol\,cm^{-3}$)
$c_{O_2}^{ref}$	reference oxygen concentration ($mol\,cm^{-3}$)
c^*	oxygen concentration at the interface of the GDL and the catalyst layer ($mol\,cm^{-3}$)
D_{O_2}	bulk diffusion coefficient of oxygen in electrolyte ($cm^2\,s^{-1}$)
$D_{O_2,GDL}$	bulk diffusion coefficient of oxygen gas ($cm^2\,s^{-1}$)
$D_{O_2,N}$	diffusion coefficient of oxygen in Nafion ($cm^2\,s^{-1}$)
$D_{O_2,W}$	diffusion coefficient of oxygen in liquid water ($cm^2\,s^{-1}$)
$D_{O_2}^{eff}$	effective diffusion coefficient for oxygen through the catalyst layer ($cm^2\,s^{-1}$)
$D_{O_2,GDL}^{eff}$	effective diffusion coefficient of oxygen in GDL ($cm^2\,s^{-1}$)
E	open circuit voltage (V)
F	Faraday's constant ($C\,mol^{-1}$)
i_0^{ref}	reference exchange current density ($A\,cm^{-2}$)
$I(x)$	proton current density at x ($A\,cm^{-2}$)
I_0	current density at a given electrode potential V_0 ($A\,cm^{-2}$)
I_{tot}	total current density in the catalyst layer ($A\,cm^{-2}$)
K_{O_2}	Henry's law coefficient (dimensionless)
L	thickness of the cathode catalyst layer (cm)
L_{GDL}	thickness of the GDL (cm)
m_{Pt}	catalyst mass loading per unit area of the catalyst layer ($g\,cm^{-2}$)
n	number of electrons transferred in cathode reaction
P_{O_2}	oxygen pressure (atm)
R	gas constant ($J\,K^{-1}\,mol^{-1}$)
T	temperature (K)
V_0	given electrode potential (V)
x	coordinate (cm)
%N	mass percentage of Nafion to the sum of Nafion and solid particles
%Pt	mass percentage of platinum catalyst on the support carbon black

Greek

α_c	cathodic transfer coefficient
α_a	anodic transfer coefficient
ε_N	volume fraction of the Nafion in the catalyst layer
ε_S	volume fraction of solid catalyst particles in the catalyst layer
ε_V	volume fraction of the void space in the catalyst layer,
ε_{GDL}	porosity of the GDL
η	overpotential (V)
σ_N	bulk conductivity of Nafion ($S\,cm^{-1}$)
σ_S	bulk conductivity of solid catalyst (platinum + carbon) ($S\,cm^{-1}$)
ρ_{Pt}	mass density of the platinum ($g\,cm^{-3}$)
ρ_C	mass density of the carbon black ($g\,cm^{-3}$)
ρ_N	mass density of Nafion ($g\,cm^{-3}$)
σ_N^{eff}	effective conductivity in Nafion ($S\,cm^{-1}$)
σ_S^{eff}	effective conductivity in solid catalyst particle ($S\,cm^{-1}$)

loading on cathode performance individually and concluded that 30 wt.% of Nafion content and $0.20 \pm 0.05\,mg/cm^2$ of platinum loading were the optimum values to obtain the best performance when 20% Pt/C catalyst was used to make the cathode. The reported best performance of 30 wt.% Nafion or $0.20 \pm 0.05\,mg/cm^2$ Pt loading seems to be local maximum, not global. They did not discuss what values the optimal Nafion content and platinum loading would be in order to obtain the best cathode performance when both Nafion content and platinum loading are variables. Boyer et al. [9] gave a set of equations to optimize the thickness, catalyst loading and Nafion content individually when only one mass

transfer process was significant, and the numerical analysis and the experimental results were compared. Marr and Li [10] performed a numerical analysis to optimize the performance of cathode and indicated that optimal ionomer content as well as an optimal void fraction exists regarding the change of the local current density with ionomer content or void fraction. In their calculation, the effective diffusion coefficient of oxygen in catalyst layer is estimated by applying the Bruggeman relation to the combination of ionomer and water in which the bulk diffusion coefficient is calculated based on a series resistance model.

This work focuses on the numerical optimization of the cathode catalyst layer with respect to one or two of the four design parameters: Nafion content, void volume fraction or porosity, thickness and platinum loading, by means of the one-dimensional "macro-homogeneous" model [3,10]. Isothermal and steady state assumptions are assumed. Oxygen diffusion is described by Fick's law. The effective diffusion coefficient of oxygen in catalyst layer is estimated as follows: first applying the Bruggeman relation to Nafion and water to obtain the effective diffusion coefficients of oxygen in Nafion and water, respectively, and then using a series resistance model. Proton migration in catalyst layer is described by the Ohm's law, and electrochemical kinetics are described by the Butler–Volmer equation.

2. Mathematical model for the catalyst layer

A schematic diagram of the cathode catalyst layer is shown in Fig. 1. Oxygen diffusion through the catalyst layer is assumed to be due to its concentration gradient, and therefore the oxygen concentration distribution is governed by Fick's law:

$$\frac{\mathrm{d}c_{\mathrm{O_2}}}{\mathrm{d}x} = \frac{I(x) - I_{\mathrm{tot}}}{nFD^{\mathrm{eff}}_{\mathrm{O_2}}} \tag{1}$$

where $c_{\mathrm{O_2}}$ is the concentration of oxygen in the catalyst layer, x the coordinate, $I(x)$ the proton current density in the catalyst layer, $I_{\mathrm{tot}} = I(L)$ the total current density in the catalyst layer, n the number of electrons transferred in the oxygen reduction reaction, and F is the Faraday's constant. $D^{\mathrm{eff}}_{\mathrm{O_2}}$, the effective diffusion coefficient for oxygen in the catalyst layer is evaluated by applying series resistance model [10] to effective diffusion of oxygen in Nafion and liquid water:

$$\frac{\varepsilon_{\mathrm{N}} + \varepsilon_{\mathrm{V}}}{D^{\mathrm{eff}}_{\mathrm{O_2}}} = \frac{\varepsilon_{\mathrm{N}}}{D^{\mathrm{eff}}_{\mathrm{O_2,N}}} + \frac{\varepsilon_{\mathrm{V}}}{D^{\mathrm{eff}}_{\mathrm{O_2,W}}} \tag{2}$$

where $D^{\mathrm{eff}}_{\mathrm{O_2,N}}$ and $D^{\mathrm{eff}}_{\mathrm{O_2,W}}$ are the effective diffusion coefficients of oxygen in Nafion and liquid water, respectively, and ε_{N} and ε_{V} are the volume fractions of Nafion and void space in the catalyst layer, respectively.

According to the model assumption that the catalyst layer is fully flooded and the void space in the catalyst layer is completely filled with water, the effective diffusion coefficients of oxygen in Nafion and water can be evaluated respectively using Bruggeman relation:

$$D^{\mathrm{eff}}_{\mathrm{O_2,N}} = D_{\mathrm{O_2,N}}\varepsilon_{\mathrm{N}}^{3/2} \tag{3a}$$

and

$$D^{\mathrm{eff}}_{\mathrm{O_2,W}} = D_{\mathrm{O_2,W}}\varepsilon_{\mathrm{V}}^{3/2} \tag{3b}$$

where $D_{\mathrm{O_2,N}}$ and $D_{\mathrm{O_2,W}}$ are the bulk diffusion coefficients of oxygen in Nafion and water, respectively.

The oxygen concentration in the catalyst layer, $c_{\mathrm{O_2}}$, is restricted by following boundary condition:

$$c_{\mathrm{O_2}}(x = 0) = c^* \tag{4}$$

where c^* is the oxygen concentration at the GDL/catalyst layer interface. Applying Fick's law for oxygen diffusion in the GDL, and solving the resulting equation, yield the following expression for c^*:

$$c^* = \frac{1}{K_{\mathrm{O_2}}}\left(\frac{P_{\mathrm{O_2}}}{RT} - \frac{I_{\mathrm{tot}}L_{\mathrm{GDL}}}{nFD^{\mathrm{eff}}_{\mathrm{O_2,GDL}}}\right) \tag{5}$$

where $P_{\mathrm{O_2}}$ is the oxygen pressure, R the gas constant, T the temperature, L_{GDL} the thickness of the GDL, and $K_{\mathrm{O_2}}$ is Henry's coefficient (dimensionless) for oxygen gas dissolved in liquid water and can be evaluated from the empirical relation [3] as

$$K_{\mathrm{O_2}} = \frac{1}{RT}\exp\left(-\frac{666}{T} + 14.1\right) \tag{6}$$

$D^{\mathrm{eff}}_{\mathrm{O_2,GDL}}$ is the effective diffusion coefficient of oxygen in GDL and can also be calculated by Bruggeman relation:

$$D^{\mathrm{eff}}_{\mathrm{O_2,GDL}} = D_{\mathrm{O_2,GDL}}\varepsilon_{\mathrm{GDL}}^{3/2} \tag{7}$$

where $D_{\mathrm{O_2,GDL}}$ is the bulk diffusion coefficient of oxygen gas and $\varepsilon_{\mathrm{GDL}}$ is the porosity of the GDL.

Applying Ohm's law to both the proton and electron transport yields the governing differential equation for the overpotential, η, in the cathode catalyst layer:

$$\frac{\mathrm{d}\eta}{\mathrm{d}x} = \left(\frac{1}{\sigma^{\mathrm{eff}}_{\mathrm{N}}} + \frac{1}{\sigma^{\mathrm{eff}}_{\mathrm{S}}}\right)I(x) - \frac{1}{\sigma^{\mathrm{eff}}_{\mathrm{S}}}I_{\mathrm{tot}} \tag{8}$$

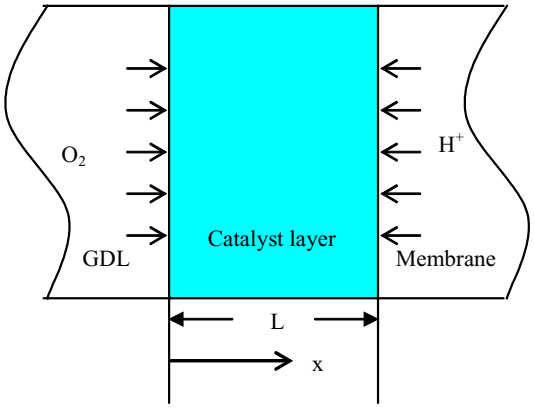

Fig. 1. The schematic diagram of the catalyst layer.

where σ_N^{eff} and σ_S^{eff} are the effective proton conductivity of Nafion and electronic conductivity of the solid catalyst particles (carbon-supported Pt), respectively, and estimated from the Burggeman relation to account for the porous nature of the cathode catalyst layer:

$$\sigma_N^{eff} = \sigma_N \varepsilon_N^{3/2} \tag{9}$$

$$\sigma_S^{eff} = \sigma_S \varepsilon_S^{3/2} \tag{10}$$

where σ_N and σ_S are the bulk proton and electronic conductivities of Nafion and solid catalyst particles, respectively. ε_S is the volume fraction of the solid catalyst particles in the catalyst layer and is given by [10]:

$$\varepsilon_S = \left(\frac{1}{\rho_{Pt}} + \frac{1 - \%Pt}{\%Pt \rho_C}\right) \frac{m_{Pt}}{L} \tag{11}$$

where ρ_{Pt} and ρ_C are the mass densities of the Pt and carbon black, respectively; %Pt represents the mass percentage of Pt catalyst supported on the carbon black; m_{Pt} is the Pt mass loading per unit area of the catalyst layer.

The sum of the Nafion volume fraction (ε_N), the void space volume fraction (ε_V) and the solid catalyst particle volume fraction (ε_S) is equal to 1:

$$\varepsilon_N + \varepsilon_V + \varepsilon_S = 1 \tag{12}$$

Combining the proton mass balance and the Butler–Volmer equation gives the equation for the proton current density:

$$\frac{dI}{dx} = A i_0^{ref} \left(\frac{c_{O_2}}{c_{O_2}^{ref}} \exp\left(\frac{\alpha_c F \eta}{RT}\right) - \exp\left(-\frac{\alpha_a F \eta}{RT}\right)\right) \tag{13}$$

where A is the specific reaction surface area per unit volume of the catalyst layer, i_0^{ref} the reference exchange current density, $c_{O_2}^{ref}$ the reference oxygen concentration, α_c and α_a are the cathodic and anodic transfer coefficients, respectively.The current density, $I(x)$, should satisfy the following boundary conditions:

$$I(0) = 0; \quad I(L) = I_{tot} \tag{14}$$

According to experimental data [11], the reference exchange current density for oxygen reduction in Nafion 117 is related with the cell temperature by [3]

$$i_0^{ref} = 10^{(3.507 - 4001/T)} \tag{15}$$

The specific reaction surface area of the catalyst layer is related to the Pt loading, m_{Pt}, and the catalyst layer thickness, L, as following:

$$A = A_0 \frac{m_{Pt}}{L} \tag{16}$$

where A_0 is the catalyst surface area per unit mass of catalyst.

3. Statement of the optimization problem

In this optimization problem, we consider the following four design variables: Nafion volume fraction (ε_N), void space volume fraction (ε_V), Pt loading (m_{Pt}) and catalyst layer thickness (L). Since PEM fuel cells are usually operated in a specific voltage range, the objective of this optimization problem is to maximize the current density at a given voltage.

Denoting the current density generated in the catalyst layer as I_0 at a given electrode potential V_0, the general optimization problem can be stated as

$$\text{Maximize} \quad I_0 \tag{17a}$$

with respect to ε_N, ε_V, L and m_{Pt}, and subject to

$$0 < \varepsilon_N < 1 \tag{17b}$$

$$0 < \varepsilon_W < 1 \tag{17c}$$

$$0 < \varepsilon_S < 1 \tag{17d}$$

and

$$\varepsilon_N + \varepsilon_W + \varepsilon_S = 1 \tag{17e}$$

where ε_S is given by Eq. (11).

The weight percentage of Nafion to the sum of Nafion and solid particles, denoted by %N, is usually used to measure the Nafion content in the electrode and can be calculated from the volume fraction as

$$\%N = \frac{\rho_N \varepsilon_N}{\rho_N \varepsilon_N + (1/\%Pt)(m_{Pt}/L)} \tag{18}$$

where ρ_N is the mass density of Nafion in liquid water.

When one parameter varies and the rest three are fixed, we have four one-parameter optimizations corresponding to the four parameters: ε_N, ε_V, L and m_{Pt}, respectively. When two of the four parameters vary and the other two are fixed, there are six two-parameter optimizations. In this paper, we will discuss the one- and two-parameter optimization problems to optimize the catalyst layer performance.

4. Numerical results and discussions

Fig. 2 gives the comparison of the experimental data [8] and the fitting current density at electrode potential $V_0 = 0.6$ V. The optimization shows that when the Nafion content is 0.32087 (here the other design parameters we: $L = 11.8\,\mu m$, $\varepsilon_V = 0.10333$, $m_{Pt} = 0.332\,mg/cm^2$), the current density at electrode potential $V_0 = 0.6$ V reaches its maximum or $0.93583\,A/cm^2$.

Fig. 3 plots the experimental data [8] and the fitting current density curve as a function of platinum loading. The highest current density is $0.71492\,A/cm^2$ when the platinum loading is $0.21032\,mg/cm^2$ which is very close to Qi and Kaufman's conclusion [8]: an optimum platinum loading is around $0.20 \pm 0.05\,mg/cm^2$.

The following section will discuss the numerical optimization analysis corresponding to one- or two-parameter optimization problems. The parameter values (baseline data)

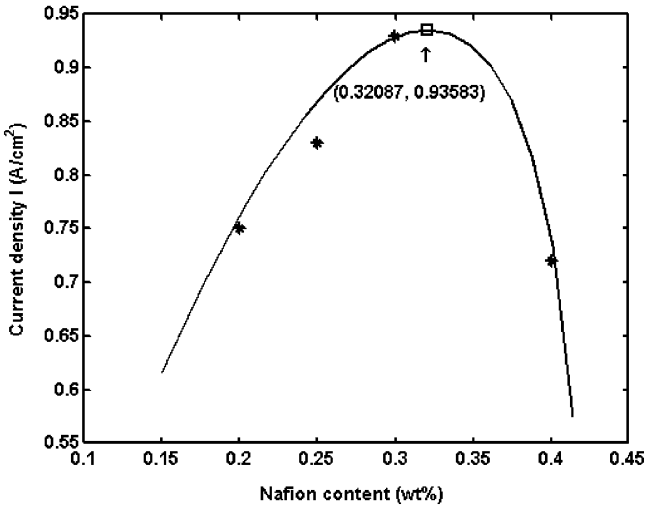

Fig. 2. Comparison of experimental data [8] and fitting result ($V_0 = 0.6$ V).

used in analysis are given in the Table 1 and the polarization curve computed using these data is shown in Fig. 4. In the process of optimization, the corresponding optimization parameter is no longer regarded as a fixed value but as a variable, satisfying the corresponding constraint conditions.

Fig. 5 gives the current density at a given electrode potential ($V_0 = 0.6$ V) as a function of Nafion volume fraction. From this figure it can be easily observed how the Nafion volume fraction affects the current density. Fig. 5 indicates the optimal Nafion volume fraction, ε_N, is 0.33619 (here $L = 11.8\,\mu$m, $\varepsilon_N = 0.08801$ and $m_{Pt} = 0.332$ mg/cm^2), and provides a maximum current density of 0.37467 A/cm^2. However, the asymmetric broadness of the plot indicates that although the current density is not very sensitive to the volume fraction near this optimal value (from 0.3 to 0.35), it is more sensitive to larger values of Nafion content than to lower values of Nafion content. For example, the current

Table 1
Parameter values used in the baseline calculation

$F = 96485$ (C mol^{-1})	$A_0 = 112 \times 10^4$ (cm g^{-1})
$R = 8.315$ (J K^{-1} mol^{-1})	$c_{O_2}^{ref} = 1.2 \times 10^{-6}$ (mol cm^{-3})
$n = 4$	$L = 1.18 \times 10^{-3}$ (cm)
$\alpha_c = 1$	$L_{GDL} = 100.0 \times 10^{-2}$ (cm)
$\alpha_a = 0.5$	$V_0 = 0.6$ (V)
$E = 1.23$ (V)	$\varepsilon_N = 0.3$
$P_{O_2} = 0.21$ (atm)	$\varepsilon_{GDL} = 0.3$
$T = 308$ (K)	$\sigma_N = 0.17$ (S cm^{-1})
$D_{O_2,GDL} = 2.396 \times 10^{-1}$ (cm^2 s^{-1})	$\sigma_S = 7.27 \times 10^2$ (S cm^{-1})
$D_{O_2,N} = 1.844 \times 10^{-6}$ (cm^2 s^{-1})	$\rho_{Pt} = 21.5$ (g cm^{-3})
$D_{O_2,W} = 3.032 \times 10^{-5}$ (cm^2 s^{-1})	$\rho_C = 2.0$ (g cm^{-3})
%Pt = 0.2	$\rho_N = 2.0$ (g cm^{-3})
$m_{Pt} = 0.332 \times 10^{-3}$ (g cm^{-2})	

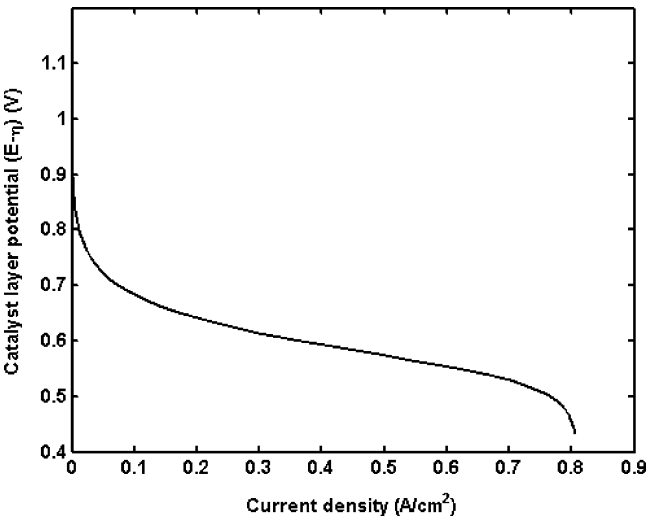

Fig. 4. Polarization curve of catalyst layer computed by using the baseline data.

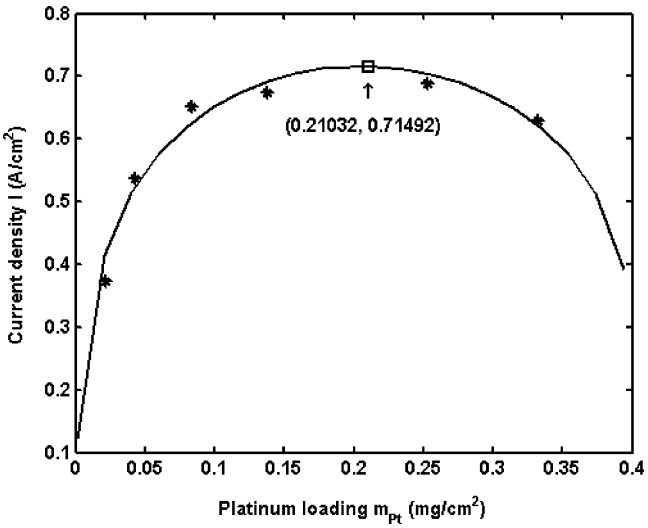

Fig. 3. Comparison of experimental data [8] and fitting result for Pt loading ($V_0 = 0.6$ V).

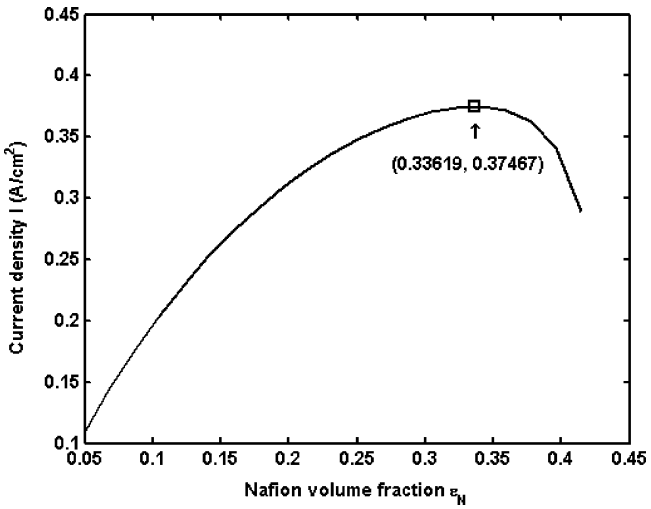

Fig. 5. Optimal point and current curve as a function of Nafion volume fraction ε_N ($V_0 = 0.6$ V).

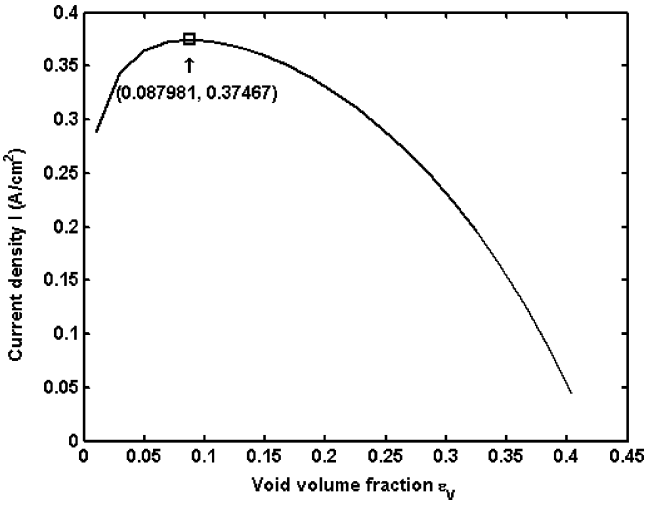

Fig. 6. Optimal point and current curve as a function of void volume fraction ε_V ($V_0 = 0.6$ V).

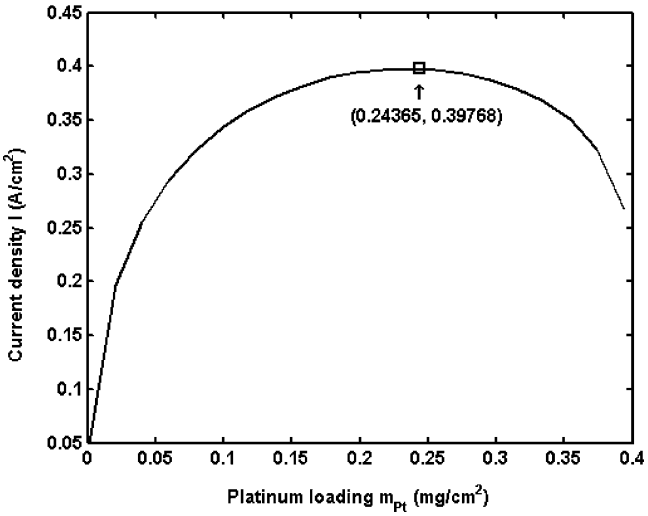

Fig. 7. Optimal point and current curve as a function of Pt loading m_{Pt} ($V_0 = 0.6$ V).

density drops by 10% when the Nafion volume fraction falls below 0.23, but the catalyst layer only tolerate up to a volume fraction of 0.4 before the current density falls below 10% of the maximum.

Fig. 6 shows the change of current density with the void volume fraction of the catalyst layer. The optimal void volume fraction ε_V, is 0.087981 (here $L = 11.8\,\mu$m, $\varepsilon_N = 0.33622$ and $m_{Pt} = 0.332$ mg/cm^2), and provides a current density of 0.37467 A/cm^2. In contrast to the case of ε_N, the dependence of the current density on ε_V, is much more sensitive to lower void volume fractions than to higher. The maximum current density in this case is exactly same with the value of the case ε_N because in both cases, the volume fraction of solid catalyst particles is a constant which means the sum of the void volume fraction and Nafion volume fraction does not change ($1 - \varepsilon_S$), so the current density as a function of void volume fraction can be regarded as the result of substitution of Nafion volume fraction by ($1 - \varepsilon_S - \varepsilon_V$) in the current density function of Nafion volume fraction.

Fig. 7 shows the relationship between current density and Pt loading. The optimal loading is 0.24365 mg/cm^2 (here $L = 11.8\,\mu$m, $\varepsilon_N = 0.3$ and $\varepsilon_V = 0.27743$), and provides a maximum current density of 0.39768 A/cm^2. The current density is not too sensitive to the Pt loading near the optimal value. A variation of about ±45% in Pt loading, leads to about 10% decrease in calculated maximum current.

The calculated current density is even more sensitive to thinner thickness of the catalyst layer than to thicker one (Fig. 8). Having a maximum value of 0.38606 A/cm^2 at optimal thickness 13.0972 μm, a variation of only 15% less than the optimal thickness, leads to 10% decrease in calculated current while a variation of 60% more than the optimal thickness leads to 10% decrease. Hence, in the design of catalyst layers, thickness needs special consideration.

Fig. 9 shows the optimal volume fractions for Nafion and void space in the two-parameter optimization when the

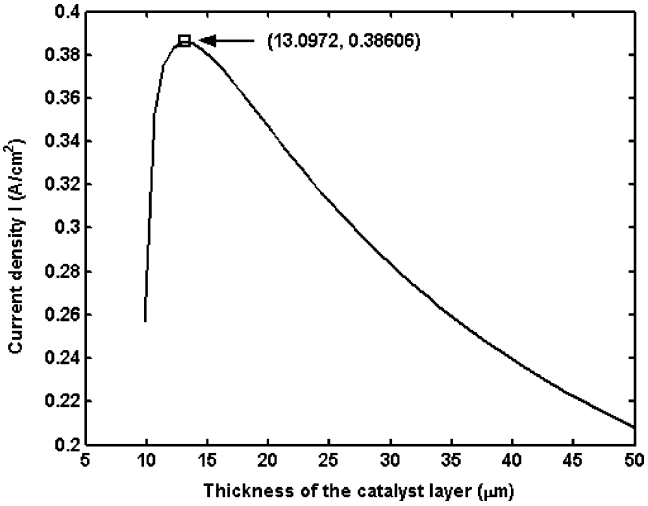

Fig. 8. Optimal point and current curve as a function of catalyst layer thickness L ($V_0 = 0.6$ V).

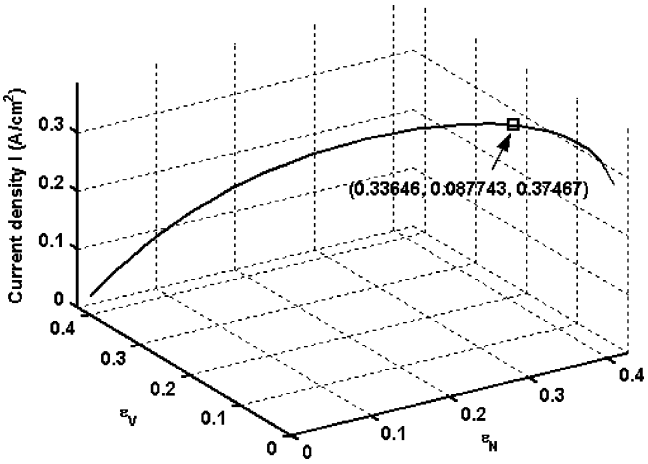

Fig. 9. Optimal point and current curve as a function of Nafion volume fraction ε_N and void volume fraction ε_V ($V_0 = 0.6$ V).

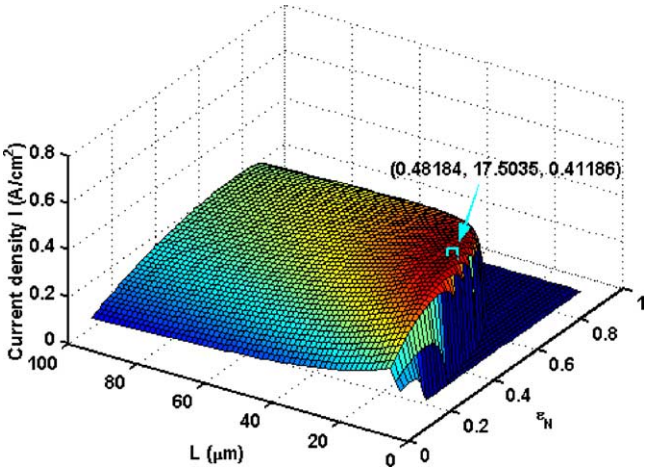

Fig. 10. Optimal point and current curve as a function of Nafion volume fraction ε_N and catalyst layer thickness L ($V_0 = 0.6$ V).

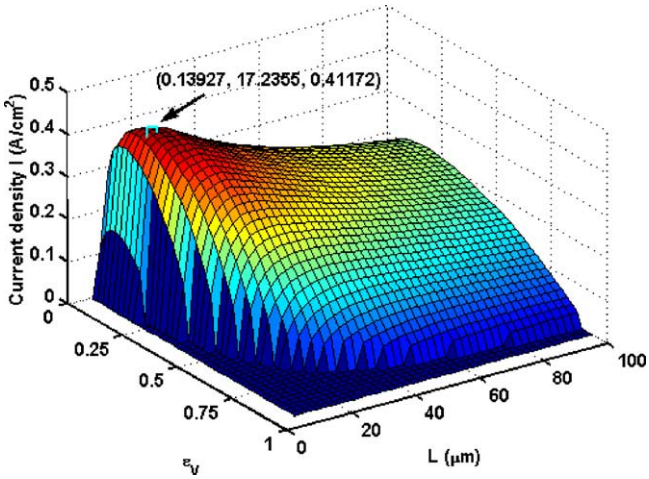

Fig. 12. Optimal point and current curve as a function of Nafion volume fraction ε_V and catalyst layer thickness L ($V_0 = 0.6$ V).

Nafion and void volume fractions are both taken into consideration. Noting that these two optimization parameters satisfy the constraint of Eq. (17e) and this equation represents a plane in the space of (ε_N, ε_V, I_{tot}) when the volume fraction of the solid catalyst particles is fixed, therefore the current density as a function of Nafion volume fraction and void volume fraction should be a curve lying in the spatial plane given by Eq. (17e), as shown in Fig. 9. The optimal current density (0.37467 A/cm^2) occurs for a Nafion volume fraction and void space volume of 0.33646 and 0.087743, respectively. These are identical to the optimal values derived for the individual one-parameter cases shown in Figs. 5 and 6 because when one parameter is taken as optimizing variable, the other varies according to Eq. (17e) in the optimization of each individual one-parameter case.

Fig. 10 shows the current density as a function of the two independent variables ε_N and L, and the corresponding optimal point for the two-parameter optimization, which occurs at (0.48184, and 17.5035 μm) and provides a maximum current 0.41186 A/cm^2. Comparing the maximum current density in Fig. 10 with those of Figs. 5 and 8, optimization of the two-parameter problem yields better results (higher current) than either of the two one-parameter optimizations.

Fig. 11 plots current density as a function of the two independent variables ε_N and m_{Pt}. An optimal point is observed from the surface figure and is calculated by the two-parameter optimization as (0.47627 and 0.19628 mg/cm^2). Comparing the maximum current density (0.44987 A/cm^2) in Fig. 11 with those in Figs. 5 and 7, the two-parameter case yields a much higher current to the two one-variable problems.

The current density as a function of void volume fraction ε_V and thickness L at a specified electrode potential ($V_0 = 0.6$ V) is given in Fig. 12. The optimal point for (ε_N, L) is (0.13927, and 17.2355 μm) and the maximum current density is 0.41172 A/cm^2.

The optimal values for void volume fraction ε_V and Pt loading m_{Pt} are 0.17616 and 0.18641 mg/cm^2, respectively,

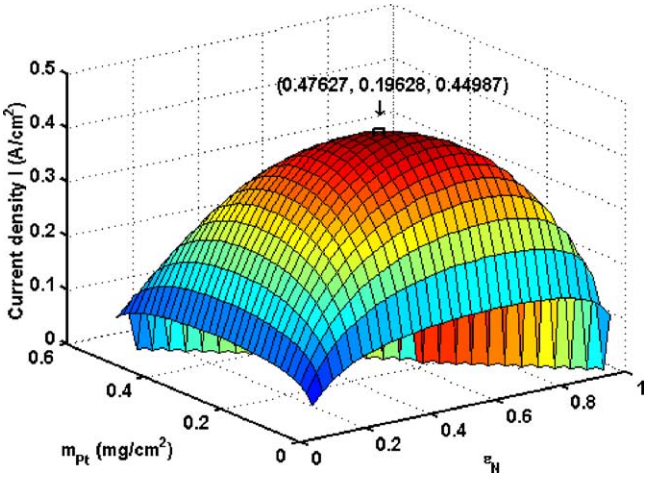

Fig. 11. Optimal point and current curve as a function of Nafion volume fraction ε_N and catalyst layer thickness m_{Pt} ($V_0 = 0.6$ V).

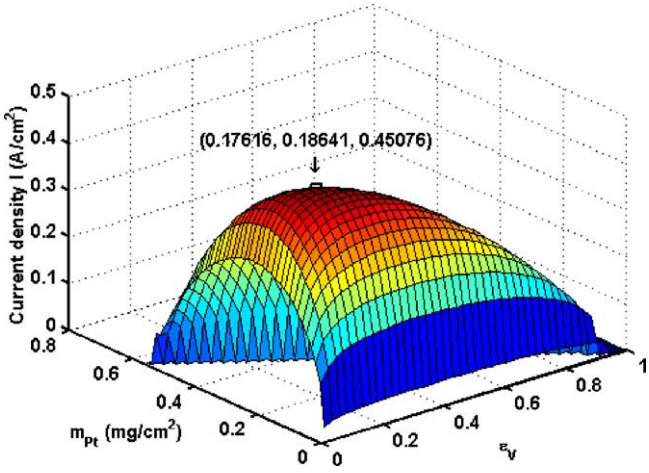

Fig. 13. Optimal point and current curve as a function of void volume fraction ε_V and catalyst layer thickness m_{Pt} ($V_0 = 0.6$ V).

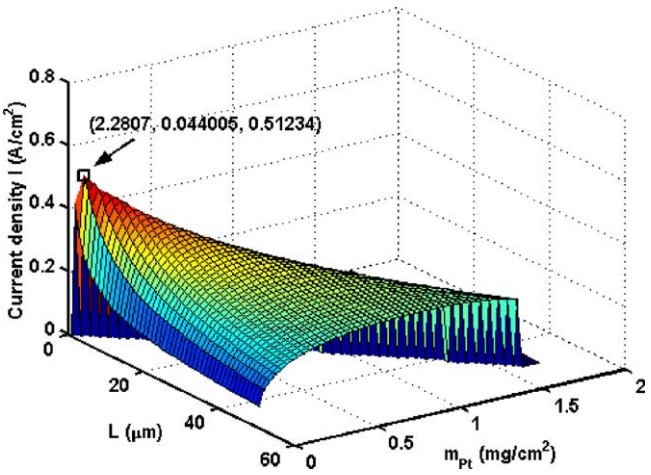

Fig. 14. Optimal point and current curve as a function of catalyst layer thickness L and catalyst layer thickness m_{Pt} ($V_0 = 0.6$ V).

and give a maximum current density of 0.45076 A/cm^2 (Fig. 13).

Fig. 14 gives the current density as a function of catalyst layer thickness L and the platinum loading m_{Pt}. A thickness of 2.2807 μm and Pt loading of 0.044 mg/cm^2 provide a maximum current of 0.51234 A/cm^2 which is much better than those in other cases above.

5. Conclusions

The design optimization problems for cathode catalyst layer are discussed numerically by taking one or two of the four design parameters (ε_N, ε_V, m_{Pt} and L) as the corresponding optimization parameter(s). Numerical analysis shows that when one of the four design parameters is taken as the optimization parameter, the corresponding one-parameter optimization always has an optimal solution. The catalyst layer performance is much more sensitive to the thickness than to the other three parameters. Additional attention should be paid to a thinner catalyst layer design in order to avoid a large drop in current density. If two of the four design parameters are taken together as the optimization parameters, the corresponding two-parameter optimization also has a global optimal solution. Numerical analysis shows that by changing the thickness and Pt loading the catalyst layer can reach its best performance compared with changing other pairs of parameters. The accuracy of the optimization problem highly depends on the accuracy of the catalyst layer model, that is, the mathematical description of the phenomena in the catalyst layer. Further theoretical and experimental studies, for example, the characterization of the relation between the effective and the bulk diffusion coefficient, oxygen diffusion in a combination of Nafion and liquid water, should be done in order to improve the optimization accuracy.

References

[1] T.E. Springer, T.A. Zawodzinski, S. Gottesfeld, Polymer electrolyte fuel cells, J. Electrochem. Soc. 138 (8) (1991) 2334–2342.
[2] T.E. Springer, M.S. Wilson, S. Gottesfeld, Modeling and experimental diagnostics in polymer electrolyte fuel cells, J. Electrochem. Soc. 140 (12) (1993) 3513–3526.
[3] D.M. Bernardi, M.W. Verbrugge, Mathematical model of a gas electrode bonded to a polymer electrolyte, AIChE J. 37 (8) (1991) 1151–1163.
[4] D.M. Bernardi, M.W. Verbrugge, A mathematical model of the solid-polymer-electrolyte fuel cell, J. Electrochem. Soc. 139 (9) (1992) 2477–2491.
[5] M. Eikerling, A.A. Kornyshev, Modeling the performance of the cathode catalyst layer of polymer electrolyte fuel cells, J. Electroanal. Chem. 453 (1998) 89–106.
[6] T. Ralph, G. Hards, J. Keating, S. Campbell, D. Wilkinson, M. Davis, J. St.-Pierre, M. Johnson, J. Electrochem. Soc. 144 (1997) 3845.
[7] M. Uchida, Y. Fukuoka, Y. Sugawara, N. Eda, A. Ohta, J. Electrochem. Soc. 143 (1997) 2245.
[8] Z. Qi, A. Kaufman, Low Pt loading high performance cathodes for PEM fuel cells, J. Power Sources 113 (2003) 37–43.
[9] C.C. Boyer, R.G. Anthony, A.J. Appleby, Design equations for optimized PEM fuel cell electrodes, J. Appl. Electrochem. 30 (2000) 777–786.
[10] C. Marr, X. Li, Composition and performance modeling of catalyst layer in a proton exchange membrane fuel cell, J. Power Sources 77 (1999) 17–27.
[11] A. Parthasarathy, S. Srinivasan, J. Appleby, Temperature dependence of the electrode kinetics of oxygen reduction at the platinum/Nafion interface: a microelectrode investigation, J. Electrochem. Soc. 139 (9) (1992) 2530–2537.